# RESOLUTION OF THE TRANSONIC FULL POTENTIAL MODEL
# BY MIXED VELOCITY-STREAM FUNCTION FINITE ELEMENTS
# AND THE ENGQUIST-OSHER NUMERICAL SCHEME.

François DUBOIS   March 1989

ECOLE POLYTECHNIQUE Centre de Mathématiques Appliquées
F-91128 Palaiseau Cedex France.

present address:   AEROSPATIALE  Division Systèmes Stratégiques
et Spatiaux, ST/MI (Direction Technique),
BP 96  F-78133 Les Mureaux Cedex France.

## ABSTRACT

We propose a new method for the numerical resolution of the full potential model of transonic flow. This method is based on a mixed finite element formulation taking into account both the velocity and the stream function of the flow and previously proposed by AMARA [1]. The nonlinearity is treated with an adaptation of the ENGQUIST-OSHER [12] numerical scheme. The complete problem is solved iteratively with the Newton's algorithm. We detail essentially the two-dimensional case and present numerical tests on a nonlifting NACA 0012 airfoil.

## -I-   INTRODUCTION

The modelling of transonic flow in the atmosphere is well known. The most important physical phenomena are the nonlinear waves of perfect gas such as the shock waves or the rarefactions. Therefore if we neglect all the viscous effects and heat transfer, the gas is a perfect fluid submitted to the Euler equations of fluid dynamics. In the following, we adopt also several hypotheses and approximations that lead to the transonic full potential model. First we restrict ourselves to stationary fluid flows. Second we suppose that the total enthalpy is constant at the upstream

infinity. Therefore the latter is constant (thanks to the Rankine-Hugoniot relations for the Euler equations) for all the points that are linked to the upstream infinity by a stream line. In the following we assume that this hypothesis is realized everywhere, i.e. that the total enthalpy is a constant. Our third hypothesis concerns the **isoentropy** and the **irrotationality** of the flow at the upstream infinity. Then this property remains true as long as the flow is regular. Moreover in transonic flow regimes the production of entropy and vorticity across the shock waves can be neglected (refer e. g. to LANDAU-LIFSCHITZ [22], SERRIN [29] or GERMAIN [13]). The fourth hypothesis concerns the thermodynamic laws satisfied by the air. Classicaly for transonic flow regimes the air is a polytropic diatomic perfect gas, then the heat capacities are two constants and their ratio $\gamma$ is equal to $7/5 = 1.4$.

We detail now the equations of this classical model. Our primitive unknown is the **velocity field**. So we first write all the equations only in terms of this field u. We introduce a reference Mach number $M_0$ and we adimensionalize the density $\rho$ and the velocity u such that $\rho=1$ and $|u|=1$ if the local Mach number M is equal to $M_0$. We get simply:

$$\rho = \left[ 1 + \frac{\gamma-1}{2} M_0^2 ( 1 - |u|^2 ) \right]^{\frac{1}{\gamma-1}} \qquad (1.1)$$

thanks to the hypothesis of isoentropy, isoenthalpy and polytropic perfect gas. The momentum q is by definition

$$q = \rho\, u \qquad (1.2)$$

It satisfies the mass-conservation law

$$\text{div } q = 0 \qquad (1.3)$$

Moreover the irrotationality condition is written simply :

$$\text{curl } u = 0 \qquad (1.4)$$

We notice that the latter equation is **exact** for two-dimensional flows around wings. Indeed lift can mathematically be produced because the domain is **not** simply connected. Then the Kutta-Joukovsky condition (the velocity remains bounded in the vicinity of the corners) allows the determiation of the lift coefficient. We refer to DJAOUA [8] for the case of incompressible two-dimensional flows. In three-dimensional situations the domain external

to a wing or a transonic glider is **simply connected** thus lift is really induced by the vorticity. In fact **curl** u is then a **measure**, even for incompressible flows. In the latter case, the vorticity is concentrated on a surface of contact discontinuity where the tangential components of u are discontinuous. We refer to HESS [18] for the formulation of the problem in those more complicated three-dimensional situations.

In this paper we restrict ourselves to twodimensional problems and in that case the equation (1.4) is valid everywhere. The usual way to re-formulate the problem (1.1)-(1.4) is to introduce the potential $\phi$ associated with the condition of irrotationality:

$$u = \mathbf{grad}\ \phi \qquad\qquad (1.5)$$

Replacing the representation (1.5) into the equations (1.1)-(1.3) we obtain the so called Transonic Full Potential Equation

$$\mathrm{div}\left\{\rho\left[\left|\mathbf{grad}\ \phi\right|^2\right]\mathbf{grad}\ \phi\right\} = 0 \qquad\qquad (1.6)$$

The density $\rho(\left|\mathbf{grad}\ \phi\right|^2)$ in the equation (1.6) is given by the formulae (1.1)-(1.5).

The numerical resolution of (1.6) with the finite difference method has been intensively studied (see e.g. JAMESON [20], CHATTOT-COULOMBEIX-DA SILVA [5], HAFEZ-SOUTH-MURMAN [17], HOLST [19] among others). Moreover approximations of the full transonic potential equation using finite element methods have been also applied with success (see e. g. BRISTEAU-PIRONNEAU-GLOWINSKI-PERIAUX-PERRIER-POIRIER [4], and HABASHI-HAFEZ [15] ).

We recall that the representation (1.5) is well adapted to irrotational velocity fields on simply connected domains. For two-dimensional lifting flows, we must add to (1.5) some special function that takes into account the possibility of lift (e.g. GIRAULT-RAVIART [14]) or we must consider $\phi$ as a multivalued function. Moreover the representation (1.5) is founded on the irrotationality condition (1.4) which is an approximation. On the other hand the conservation of the mass (1.3) is **exact** for general stationary Euler or Navier-Stokes equations. This remark motivates the introduction of the stream function $\psi$ satisfying

$$q = \mathbf{curl}\ \psi \qquad\qquad (1.7)$$

The major problem arising when we use this representation is due to the determination of the density. For transonic flows where (1.1) is valid, the density is **not** a function of the momentum **q** (see Figure 1). Thus the equation (1.4) cannot be rewritten as a single equation involving **only** the stream function as an unknown. This double root problem (discussed in detail by SELLS [28]) has been solved previously by HAFEZ-LOVELL [16] with finite differences and by AMARA [1] (see also AMARA-JOLY-THOMAS [2]) thanks to a **mixed finite element formulation**. The present work is an extension of the method proposed in [1].

In the second section of this paper we recall the discrete mixed finite element formulation for two-dimensional transonic flows governed by the equations (1.1)-(1.4) and (1.7). In Section III we detail our treatment of the nonlinear terms, based on the upwind ENGQUIST-OSHER [12] numerical scheme. The first numerical tests of the method for a non-lifting NACA 0012 profile at various Mach numbers at infinity are presented in Section IV.

## -II- VELOCITY-STREAM FUNCTION MIXED FORMULATION
### FOR TRANSONIC POTENTIAL FLOWS.

### 1) Discretization spaces

We consider a bounded domain $\Omega$ of $R^2$ and a mesh $T_h$ composed by quadrangular finite elements (the extension to triangular meshes is straightforward). The velocity **u** is supposed to be constant in each element K :

$$u \in Q_0^h \times Q_0^h \tag{2.1}$$

The discrete space $Q_0^h$ is generated by discontinuous piecewise constant functions on each finite element :

$$Q_0^h = \left\{ w : \Omega \rightarrow R, \ w|_K \in R \ , \ \forall \ K \in T_h \right\} \tag{2.2}$$

This choice implies that the numerical accuracy is at best of first order. The stream function $\Psi$ is dicretized by bilinear continuous finite elements:

$$\Psi|_K \in Q_1(K) \quad , \ \forall \ K \in T_h \tag{2.3}$$

The space $Q_1(K)$ is defined as follows. Let $K_0$ be the unity square $[0,1] \times [0,1]$ and $Q_1(K_0)$ be the following space of polynomial functions :

$$Q_1(K_0) = \left\{ w_0: K \to R , \exists\ a,b,c,d \in R,\ w_0(x,y) = a + bx + cy + dxy \right\} \quad (2.4)$$

Given a quadrangle K there exists a unique function $F_K \in Q_1(K_0)$ applying $K_0$ onto K, and we set

$$Q_1(K) = \left\{ w: K \to R,\ \exists\ w_0 \in Q_1(K_0),\ w(x,y) = w_0(\ F_K^{-1}(x,y)),\ \forall (x,y) \in K \right\} \quad (2.5)$$

For more details about this classical isoparametric quadrangle we refer to CIARLET [6].

We suppose also that we have decomposed the boundary $\Gamma \equiv \partial\Omega$ of the domain into two parts:

$$\Gamma = \Gamma_D \cup \Gamma_N \quad (2.6)$$

The portion $\Gamma_D$ corresponds to a Dirichlet boundary condition for the stream function $\Psi$: then we introduce the set $\overline{Q}_1^D$ of the continuous functions satisfying (2.3) in each element K of $T_h$, and that are null for all the vertices of the mesh $T_h$ that are not lying on $\Gamma_D$. Conversely we set

$$Q_1^h = \left\{ \varphi:\ \Omega \to R\ \text{continuous},\ \varphi|_K \in Q_1(K)\quad \forall\ K \in T_h,\ \varphi(x)=0\quad \forall\ x \in \Gamma_D \right\} \quad (2.7)$$

The stream function finally satisfies:

$$\overline{\Psi} \in \overline{Q}_1^D\quad,\quad \Psi - \overline{\Psi} \in Q_1^h \quad (2.8)$$

The integer $N_e$ (resp $N_s$) denotes the number of elements (resp vertices that are not lying on $\Gamma_D$) of the mesh $T_h$. The dimension of the discretization space $Q_0^h \times Q_0^h$ associated with the velocity (resp $Q_1^h$ associated with the stream function) is $2.N_e$ (resp $N_s$).

## 2) Nonlinear mixed formulation

We first detail the discretization of the momentum $q$ introduced in (1.2). We choose $q$ as a nonlinear function of the pair $(u,\Psi)$ whose value is supposed to be constant in each finite element:

$$q = q(u,\Psi)\quad \in\ Q_0^h \times Q_0^h \quad (2.9)$$

The dependance of the momentum (2.9) towards the stream function is realized by the choice of an **upwind element** KA(K) for each element K, as follows. Let $K_1, K_2, K_3, K_4$ be the four quadrangles of $T_h$ neighbouring the given element K (see Figure 2). The mass flux entering into K from the element $K_j$ (j=1 to 4) is exactly equal to the difference $\Psi_{i_{j+1}} - \Psi_{i_j}$ of the stream function between the vertices $i_{j+1}$ and $i_j$ defining the interface $K_j$-K. The upwind element KA(K) is defined as the one realizing the maximum of this mass-flux among the four neighbouring elements.

$$\Psi_{i_{KA(K)+1}} - \Psi_{i_{KA(K)}} \geq \sup_{j=1,2,3,4} \left[ \Psi_{i_{j+1}} - \Psi_{i_j} \right] \qquad (2.10)$$

With this choice, the direction KA(K) $\rightarrow$ K follows approximately the flow field. Moreover the criterium (2.10) is easy to implement once the stream function is known.

When the function KA(K) is determined for all the elements of the mesh, the momentum is a nonlinear function of both the velocities $u_K$ and $u_{KA(K)}$ in the quadrangles K and KA(K) respectively:

$$q(u,\Psi)\big|_K = Q(u_{KA(K)}, u_K) \quad , \quad \forall K \in T_h \qquad (2.11)$$

The choice of the function Q(.,.) will be detailed in the next sub-section.

Therefore, we can now give the mixed variational formulation of the discrete problem. The boundary conditions are of two types: the stream function is supposed to be given on $\Gamma_D$:

$$\Psi = \overline{\Psi} \text{ on } \Gamma_D \quad , \quad \overline{\Psi} \text{ given in } \overline{Q}_1^D \qquad (2.12)$$

and on the part $\Gamma_N$, we suppose that the tangential component of the velocity is given :

$$u.t = g \quad \text{on} \quad \Gamma_N \qquad (2.13)$$

where t is the unity vector tangent to $\partial\Omega$ and issued from the external normal n by a rotation of angle $+\pi/2$ (see Figure 5). Thus we multiply the representation (1.7) by a test function v in $Q_0^h \times Q_0^h$ and integrate on the domain $\Omega$. We obtain

$$\int_\Omega q(u,\Psi).v \, dx - \int_\Omega \text{curl}\Psi.v \, dx = 0 \quad , \quad \forall v \in Q_0^h \times Q_0^h \qquad (2.14)$$

Moreover, we multiply the equation (1.4) by a scalar test function $\varphi$ lying in $Q_1^h$. Integrating by parts and using (2.13) we get:

$$\int_\Omega u.curl\ \Psi\ dx\quad +\quad \int_{\partial\Omega} \varphi\ g\ d\gamma\quad =\ 0\ ,\quad \forall\ \varphi \in Q_1^h \qquad (2.15)$$

The discrete **nonlinear mixed variational formulation** for solving the transonic problem in the domain $\Omega$ takes the form:

*Find a pair (u,$\Psi$) satisfying the functional relations (2.1) and (2.8) repectively and the variational equations (2.14)(2.15).*

We recall that this problem is entirely defined by the data $(\overline{\Psi},g)$ related to the boundary conditions (2.8) and (2.13) and by the nonlinear dependance of the momentum towards the velocity described by the formula (2.11).

We introduce some definitions. For $\varphi$ lying in the discrete space $Q_1^h + \overline{Q}_1^D$, the vector $B\varphi$ belongs to $Q_0^h \times Q_0^h$ and is defined by

$$\int_\Omega B\varphi.v\ dx\ =\ -\int_\Omega curl\varphi.v\ dx \qquad \forall\ v \in Q_0^h \times Q_0^h \qquad (2.16)$$

We define G as the line vector of order $N_s$ such that

$$G\varphi \qquad = \int_\Gamma g\ \varphi\ d\gamma \qquad \forall\ \varphi \in Q_1^h \qquad (2.17)$$

and vol(K) as the Lebesgue measure of K:

$$vol(K) \qquad = \int_K dx \qquad \forall\ K \in T_h \qquad (2.18)$$

We re-write the problem (2.14)-(2.15) thanks to these notations:

$$\left\{ \begin{array}{l} u \in Q_0^h \times Q_0^h\ ,\quad \Psi - \overline{\Psi} \in Q_1^h \\ vol(K)\ Q(u_{KA(K)},u_K)\quad +\ B\Psi\ =\ 0 \\ {}^tBu \qquad\qquad\qquad\qquad = G \end{array} \right. \qquad (2.19)$$

The notation ${}^tB$ denotes the transpose of the (rectangular) matrix B. The problem (2.19) is nonlinear but we recognize the typical pattern of the mixed formulations (e.g. BREZZI [3]).

Remark 2.1. This formulation (2.19) can be extended for three-dimensional problems. The velocity u remains constant in each element (tetrahedron, prism or hexahedron) and the vector potential $\Psi$ is dicretized with the finite element introduced by NEDELEC [25]. In [9] we have analysed theoretically a linear problem formulated with a mixed formulation of the type (2.19). On the other hand DUBOIS-DUPUY have presented in [10] a three-dimensional transonic flow simulation using that type of mixed formulation and a determination of the flux function $Q(u_{KA}, u_K)$ founded on an upwinding of the density which is described in the next section.

## 3) Nonlinear evaluation of the momentum.

We detail in this section the way to compute the momentum (2.11) in a finite element K as soon as the upwind element KA is known. Since the pioneering work of EBERLE [11], the upwinding of the density is well known. We write it in terms of the momentum:

$$Q(u_{KA}, u_K) = \bar{\rho}(u_{KA}, u_K) \cdot u_K \qquad (2.20)$$

with an upwind density $\bar{\rho}$ evaluated thanks to the scheme

$$\bar{\rho}(u_{KA}, u_K) = \alpha_{KA,K} \, \rho_{KA} + (1-\alpha_{KA,K}) \, \rho_K \qquad (2.21)$$

The values $\rho_{KA}$ and $\rho_K$ are computed from the moduli of the associated velocities with help of (1.1). The coefficient $\alpha_{KA,K}$ can be found in BRISTEAU et al [4], HAFEZ-SOUTH-MURMAN [17], or HOLST [19] and we have used the formula proposed by AMARA [1]. Our present scheme is based on the upwinding of the momentum itself and can be viewed as an adaptation of the ENGQUIST-OSHER [12] scheme to the transonic full potential problem. This kind of adaptation was previously proposed by OSHER-HAFEZ-WHITLOW [26] for the full potential equation (1.16) in the context of finite differences.

We suppose for a while that the velocities $u_{KA}$ and $u_K$ are normal to the interface separating the elements KA and K. The evolution in time of the density is then locally described by the nonlinear scalar concave hyperbolic equation

$$\frac{\partial\rho}{\partial t} + \frac{\partial}{\partial x}\left\{ \rho\left[ 1+ \frac{2}{(\gamma-1)M_0^2}(1-\rho^{\gamma-1})\right]^{1/2} \right\} = 0 \qquad (2.22)$$

associated with the initial datum (Figure 2.3)

$$\rho_0(x) = \begin{cases} \rho_{KA} & , \ x < 0 \\ \rho_K & , \ x > 0 \ . \end{cases} \qquad (2.23)$$

The system (2.22)(2.23) is a **Riemann problem** associated with the scalar conservation law (2.22). The solution $\rho(x,t)$ is self-similar and therefore remains constant at the interface between KA and K along the time evolution (see e.g. LAX [23] or SMOLLER [30] for the mathematical foundations of the hyperbolic conservation laws). The numerical scheme proposes an approximate computation (denoted by $\phi$) of the flux function associated with the conservation law (2.22) for x/t=0. Under the hypothesis made previously on the velocity vectors $u_{KA}$ and $u_K$, the numerical flux corresponds to the modulus of the momentum $Q(u_{KA},u_K)$. Therefore we have

$$\left| Q(u_{KA},u_K) \right| = \phi(u_{KA},u_K) \tag{2.24}$$

The numerical flux characterizes the choice of the nonlinear numerical scheme. We detail at the end of this section the adaptation of the ENGQUIST-OSHER scheme to the conservation law (2.22). When the flow is aligned with the direction of the interface separating KA and K, the modulus computed thanks to (2.24) is exactly the component of the momentum Q in the direction normal to the interface (Figure 3). In the general case, our choice of the upwinding element KA(K) assumes that the direction KA-K is not far from the direction of the flow, which is given in the element K by the velocity $u_K$. Thanks to these phenomenological considerations we define our momentum function by:

$$Q(u_{KA},u_K) = \phi(u_{KA},u_K) \frac{u_K}{|u_K|} \qquad \text{in } K \in T_h \tag{2.25}$$

The definition of our nonlinear treatment will be complete after having specified the function $\phi(.,.)$ related to the Engquist-Osher scheme. We first write the flux of the equation (2.22) in terms of the velocity:

$$q(u) = \left[ 1 + \frac{\gamma-1}{2} M_0^2 (1-|u|^2) \right]^{\frac{1}{\gamma-1}} |u| \tag{2.26}$$

and following [12], we split it into a supersonic part g(u) plus a subsonic part e(u):

$$g(u) = \begin{cases} 0 & |u| \leq u_s \\ q(u) - Q_{max} & |u| \geq u_s \end{cases} \tag{2.27}$$

$$e(u) = \begin{cases} q(u) & |u| \leq u_s \\ Q_{max} & |u| \geq u_s \end{cases} \tag{2.28}$$

The parameters $Q_{max}$ and $u_s$ are defined on the Figure 4 and are easily evaluated from the equation (2.26). Then the numerical flux function is defined by

$$\phi(u_{KA}, u_K) = g(u_{KA}) + e(u_K) \ .$$  (2.29)

## -III - QUASI-NEWTON ALGORITHM FOR THE NUMERICAL RESOLUTION.

The discrete problem (2.19) that results from the mixed variational formulation couples the unknowns u and $\Psi$. We note that the flux function $Q(u_{KA(K)}, u_K)$ is defined thanks to the choice of the upwind element KA(K) related to the value of the stream function $\Psi$. We remark also that KA(K) is not derivable towards the stream function field. In the following, we suppose that the upwind element KA(K) associated with each finite element K is **fixed**. More precisely the direction of the flow is supposed to be sufficiently well known in order to be sure that the upwind element KA(K) remains the same during the iterations of the algorithm. Therefore the momentum $Q(u_{KA(K)}, u_K)$ is considered in the following only as a function of the **velocity** field.

We introduce the notations

$$X \equiv (u, \zeta) \ \in \ (Q_0^h)^2 \times Q_1^h$$  (3.1)

$$F(X) = \begin{bmatrix} \text{vol}(K) \ Q(u_{KA(K)}, u_K) \ + \ B(\zeta + \bar{\Psi}) \\ {}^t Bu \ - \ G \end{bmatrix}$$  (3.2)

Then F is a $C^1$ function of the unknown X which takes its value in the space $(Q_0^h)^2 \times Q_1^h$ (the first line of F(X) must be considered element by element) and the equation (2.19) takes the simple algebraic form:

$$F(X) = 0$$  (3.3)

We have used a classical Newton's algorithm for the numerical resolution of the nonlinear equation (3.3):

$$\begin{cases} X^0 \ \text{given in} \ (Q_0^h) \times (Q_1^h) & (3.4) \\ dF(X^m).\delta X \ + \ F(X^m) \ = 0 & (3.5) \\ X^{n+1} \ = \ X^n + \omega^n \ \delta X & (3.6) \end{cases}$$

In the equation (3.5) $dF(X^m)$ denotes the jacobian matrix of the function F,

evaluated at the $m°$ iteration; we have updated this matrix every 10 iterations, i.e. we have taken in (3.5) the following value for m :

$$m = 1 + 10*integer\ part(\frac{n}{10}) \qquad (3.7)$$

The relaxation factor $\omega^n$ in the equation (3.6) is computed thanks to the relations

$$\begin{cases} 0 \le \omega^n \le 1 \\ \omega^n \displaystyle\max_{K \in \mathcal{T}_h} |\delta u_K| \le 0.01 \end{cases} \qquad (3.8)$$

where $\delta u_K$ denotes the increment of the velocity field inside the finite element K associated with the increment $\delta X \equiv (\delta u, \delta \Psi)$. To be complete, we precise that the value of the reference Mach number $M_0$ (cf the equations (1.1) and (2.26)) has been chosen as a constant for all the computations:

$$M_0 \equiv 1 \qquad (3.9)$$

The matrix dF(X) around the state $X \equiv (u, \Psi - \overline{\Psi})$ is sparse. The first $2*N_e$ lines correspond to the coupling (2.14) of each element K with itself (diagonal $2*2$ blocks $\partial Q/\partial u_K$), with its upwind element KA (nondiagonal $2*2$ block $\partial Q/\partial u_{KA}$) and with the (four) vertices neighbouring K (B block that takes into account the degrees of freedom related to the stream function). The last $N_s$ lines result from the equation (2.15) and couples each vertex with the velocity vectors inside the four neighbouring elements (block associated with the transpose of the matrix B).
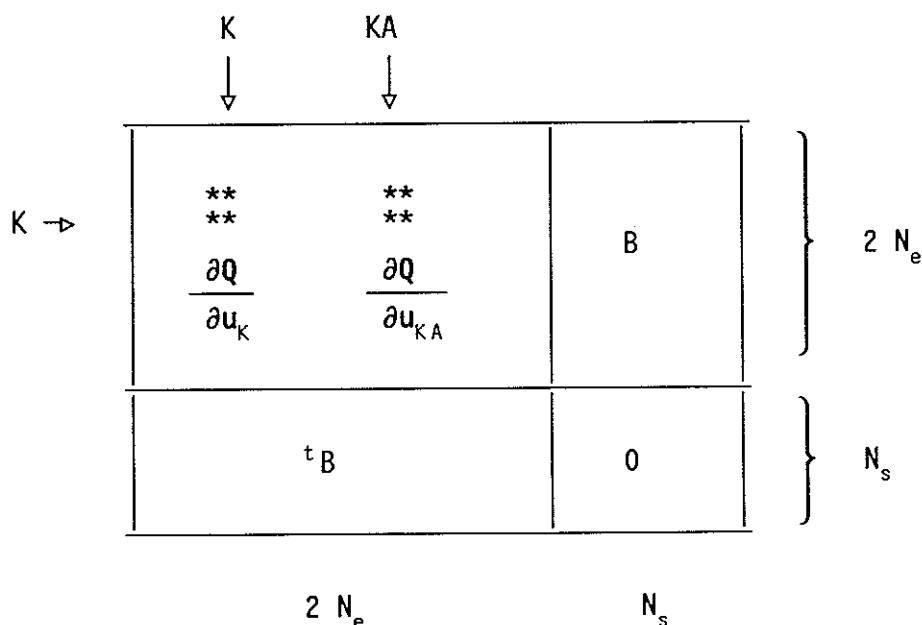
The linear system (3.5) is *a priori* difficult to inverte. The null $N_s * N_s$ block assures that $dF(X^m)$ is neither diagonally dominant nor positive definite (i.e. $(dF(X^m).y,y) > 0$, $\forall y \neq 0$ ). For instance, conjugate gradient methods are applicable only if a good preconditioning technique has been devised (see e.g. JOLY [21]). So we have chosen to inverte the linear system (3.5) according to an exact L.U factorization (with pivoting) of the matrix $dF(X^m)$ (routine F01BRF of the NAG [24] library).

We specify now the expression of the 2x2 matrices $\partial Q/\partial u_{KA}$ and $\partial Q/\partial u_K$. Let us denote by $\chi(s)$ the Heaviside function

$$\chi(s) = \begin{cases} 1 & s \geq 0 \\ 0 & s < 0 \end{cases} \tag{3.11}$$

For L equal to K or KA(K) we denote by $\rho_L$ (resp $c_L$, $u_L$, $v_L$) the density (resp sound velocity, x and y components of the velocity $u_L$) inside the element L.

$$\begin{cases} u_L = (u_L, v_L) \\ \rho_L = \rho(u_L) \\ c_L = \sqrt{\dfrac{1}{M_0^2} \rho_L^{\gamma-1}} \end{cases} \tag{3.12}$$

We derive the expression (2.25) towards $u_{KA}$ and $u_K$. We obtain easily

$$\frac{\partial Q}{\partial u_{KA}} = \frac{\rho_{KA}}{|u_K|} \frac{\chi(|u_{KA}|-c_{KA})}{|u_{KA}|} \left( 1 - \frac{|u_{KA}|^2}{c_{KA}^2} \right) \begin{bmatrix} u_K u_{KA} & u_K v_{KA} \\ v_K u_{KA} & v_K v_{KA} \end{bmatrix} \tag{3.13}$$

and

$$\frac{\partial Q}{\partial u_K} = \frac{\rho_K}{|u_K|^2} \chi(c_K-|u_K|) \left(1 - \frac{|u_K|}{c_K}\right) \begin{bmatrix} u_K^2 & u_K v_K \\ u_K v_K & v_K^2 \end{bmatrix} +$$

$$+ \frac{\phi(u_{KA}, u_K)}{|u_K|^2} \begin{bmatrix} v_K^2 & -u_K v_K \\ -u_K v_K & u_K^2 \end{bmatrix}$$

$$\tag{3.13}$$

## -IV - NUMERICAL TESTS ON THE NACA 0012 PROFILE

### 1) Generalities

We present in this section the first numerical results obtained with the method described above. We have chosen the classical NACA 0012 profile in non-lifting configurations (lifting test cases can be produced with the same formulation and analogous boundary conditions, thank to the use of a stream function rather than a scalar potential as we mentioned in the introduction). The boundary conditions (2.12)(2.13) are specified on the figure 5. The mesh used for the computations is displayed on the figure 6; it contains 350 elements and 21 points on the airfoil. It is a relatively coarse mesh but the order of the associated matrix dF(X) (cf equation (3.5)) is

$$2 \text{ NE} + \text{NS} \simeq 2*350 + 360 = 1060 \qquad (4.1)$$

This order has been practically the maximum admissible to get interesting numerical results in a reasonable computing time. The initial state (3.4) corresponds to the uniform flow at infinity for classical values of the infinite Mach number : 0.80, 0.85, 0.90, 0.95, 1.20. On the other hand, for the values 1.00, 1.05, 1.10 of the upstream Mach number, we have chosen the initial state as the solution of the previous test case. The machine accuracy (Cray2 computer) has been obtained after 200 nonlinear iterations of the Newton algorithm (this corresponds to 20 L*U factorizations). A typical evolution of the residual

$$\epsilon_n = \max_{K \in T_h} |\rho_K^{n+1} - \rho_K^n| / \max_{K \in T_h} |\rho_K| \qquad (4.2)$$

is presented on Figure 7.

### 2) Analysis of a first family of test cases

The test cases at $M_\infty = 0.80$ and 0.85 are classical (refer e.g. to the different contributions in RIZZI-VIVIAND [27], and to BRISTEAU et al [4]). The isomach curves are displayed on the Figures 8 and 9. The jumps on the discrete shock waves corresponds to the values given by the authors of [27], as we can see on the Figure 12.

The case $M_\infty = 0.90$ presents an oblique shock wave attached to the trailing edge of the airfoil (Figure 10). Our results are comparable with those presented previously by BRISTEAU et al [4]. A fishtail shock is present when $M_\infty = 0.95$. This kind of structure characterizes the transonic flow fields when the Mach number is close to one; it has been observed previously by JAMESON and HOLST in [27] and by HABASHI-HAFEZ [15]. Our result (Figure 11) contains also a fishtail shock wave , and this fact was not *a priori* expected. Indeed the hypotheses done when we have derived the numerical scheme (2.29) are clearly not realized in an oblique shock. On the other hand, the location of the secondary straight shock wave is varying with the authors [27,15]. Our value corresponds to 0.5 times the chord downstream to the trailing edge of the profile, that is comparable with the value given previously by HABASHI-HAFEZ [15].

A supersonic upstream value ($M_\infty = 1.20$) for the Mach number has been presented by HABASHI-HAFEZ [15] and OSHER-HAFEZ-WITHLOW [26]. We observe a detached shock wave located 0.4 times the chord upstream to the leading edge as in [15,26]. This wave is smeared by our mesh width, particularly coarse in this region (Figure 13).

Our results on the classical test cases presented in this section show the great possibilities of the numerical scheme. The formulation is robust and admits subsonic as well as supersonic upstream Mach numbers.

## 3) New test cases

The upstream Mach numbers 1.00, 1.05, 1.10 on a NACA 0012 airfoil have not been proposed previously at our knowledge. The test at $M_\infty = 1.00$ is particularly singular. On the one hand the mathematical type of the linearized problem is parabolic (rather than elliptic when $M_\infty < 1$ and hyperbolic when $M_\infty > 1$).
On the other hand the initialization of the computation in the whole domain by the uniform value of the flow at infinity leads to a singular matrix in the equation (3.5). This fact is due to the singularity of the 2x2 matrices $\partial Q/\partial u_K$ and $\partial Q/\partial u_{KA}$ (formulae (3.12)(3.13)) when

$$u_K = (c_K,0) \quad , \quad \forall \; K \in T_h \tag{4.3}$$

This numerical condition expresses the parabolicity of this flow. Thus we have initialized this test case by the solution of the case $M_\infty = 0.95$ as we have mentioned in Section 1. No particular numerical problem has arisen

and the results are displayed on Figure 14. The Figures 15 and 16 present the isomach curves in the domain for the cases at $M_\infty$ = 1.05 and 1.10. The Figure 17 shows the same field along the profile and the line following the trailing edge. In the three cases, a fishtail shock is present and its structure is growing up with the parameter $M_\infty$. The bow shock becomes visible at $M_\infty$ = 1.10 (Figure 16) and for $M_\infty$ = 1.05 this wave is captured on our mesh. In the limiting case ($M_\infty$ = 1.00) no bow wave exists (according to COLE-COOK [7]). All those results are qualitatively correct if we refer to the previous work of JAMESON [20] on the 65.15.10 airfoil for infinite upstream Mach numbers around 1.

## CONCLUSION

For the numerical resolution of the full potential model of transonic flows, we have proposed a nonlinear formulation involving both a mixed finite element method, a stream function and an upwinding of the momentum based on the ENGQUIST-OSHER [12] scheme. The main point of this formulation is a strong coupling between the velocity and the stream function involving a very large matrix of mixed type in the Newton iterations of the algorithm. This fact actually limits the method to coarse meshes in twodimensional problems. Nevertheless a wide range of infinite upstream Mach numbers (0.80 to 1.20 including flows at Mach 1) has been applied with success to a nonlifting NACA 0012 airfoil.

## ACKNOWLEDGMENT

## REFERENCES

1   AMARA M., Analyse de Méthodes d' Elements Finis pour des Ecoulements Transsoniques, Thèse d' Etat, Paris 6 University (1983).

2   AMARA M., JOLY P., THOMAS J.M., A Mixed Finite Element Method for Solving Transonic Flow Equations, Comp. Meth. Appl. Mech. Eng., vol 39 (1983), pp 1-18.

3   BREZZI F. On the Existence, Uniqueness and Approximations of Saddle Point Problems Arising from Lagrangian Multipliers, RAIRO, vol 2, (1974) , pp 217-235.

4   BRISTEAU M.O., PIRONNEAU O., GLOWINSKI R., PERIAUX J., PERRIER P., POIRIER G., On Numerical Solution of Nonlinear Problems in Fluid Dynamics by Least Squares and Finite Element Method (II): Application to Transonic Flow Simulations, Comp. Meth. Appl. Mech. Eng., vol 51 (1985), pp 363-394.

5   CHATTOT J.J., COULOMBEIX C., da SILVA TOME C. Calculs d'écoulements transsoniques autour d'ailes, la Recherche Aérospatiale, n° 1978-4, pp 143-159.

6   CIARLET P., The Finite Element Method for Elliptic Problems, North Holland, Amsterdam (1978).

7   COLE J., COOK P., Transonic Aerodynamics, North Holland Series in Applied Mathematics and Mechanics, Amsterdam (1986).

8   DJOUA M., A Method of Calculation of Lifting Flows Around Two-Dimensional Corner-Shaped Bodies, Math. of Comp., vol 36, n° 154 (1981), pp 405-425.

9   DUBOIS F., Discrete Vector Potential Representation of a Divergence Free Vector Field in Three Dimensional Domains: Numerical Analysis of a Model Problem, Internal Report n° 163 (june 1987), Centre de Mathématiques Appliquées de l'Ecole Polytehnique, to appear in SIAM J. of Numerical Analysis.

10  DUBOIS F., DUPUY J.M., A Three Dimensional Vector Potential Formulation for Solving Transonic Flow with Mixed Finite Elements, in 6° Int. Conf. on Finite Elements in Fluids, Antibes (1986).

11  EBERLE A. Eine Method Finiter Elements Berechnung der Transsonicken Potential-Strimung um Profile, Messerschmitt-Bölkow-Blohm, (1977), n° 1352(o).

12  ENGQUIST B., OSHER S., Stable and Entropy Satisfying Approximatios for Transonic Flow Calculations, Math. of Comp., vol 34, n° 149 (1980), pp 45-75.

13  GERMAIN P., Cours de Mécanique de l'Ecole Polytechnique, Ellipses, Paris (1986).

14  GIRAULT V., RAVIART P.A., Finite Element Methods for Navier-Stokes Equations, Theory and Applications, Springer Verlag, Berlin (1986).

15  HABASHI W., HAFEZ M., Finite Element Solutions of transonic Flow Problems, AIAA J., vol 20, n° 10 (1982), pp 1368-1376.

16  HAFEZ M., LOVELL D., Numerical Solution of Transonic Stream Function, AIAA J., vol 21, n° 3 (1983), pp 327-335.

17  HAFEZ M., SOUTH J., MURMAN E. Artificial Compressibility Methods for Numerical Solutions of Transonic Full Potential Equation, AIAA J., vol 17, n° 8 (1979), pp 838-844.

18  HESS J., The Problem of Three-Dimensional Lifting Potential Flow and its Solution by means of Surface Singularity Distribution, Comp. Meth. Appl. Mech. Eng., vol 4 (1974), pp 283-319.

19  HOLST T., Implicit Algorithm for the Conservative Transonic Full Potential Equation Using an Arbitrary Mesh, AIAA J., vol 17 (1979), pp 1038-1045.

20  JAMESON A., Iterative Solution of Transonic Flows over Airfoils and Wings, Including Flows at Mach 1, Comm. Pure Appl. Math., vol 27 (1974), pp 283-309.

21  JOLY P. Présentation de synthèse des méthodes de gradient conjugué, Math. Modelling and Numer. Anal., vol 20, n° 4 (1986), pp 639-665.

22  LANDAU L., LIFCHITZ E. Mécanique des Fluides, Mir Editions, Moscou (1953,1971).

23  LAX P., Hyperbolic Systems of Conservation Laws and the Mathematical Theory of Shock Waves, CBMS Regional Conf. Series in Applied Maths., SIAM Philadelphia (1973).

24  N.A.G., Numerical Algorithm Group, NAG Fortran Library Manual, Oxford (1982).

25  NEDELEC J.C. Mixed Finite Elements in $R^3$, Numer. Math., vol 35 (1980), pp 315-341.

26  OSHER S., HAFEZ M; WHITHLOW W., Entropy Condition Satisfying Approximations for the Full Potential Equation of Transonic Flow, Math. of Comp., vol 44 (1985), pp 1-29.

27  RIZZI A., VIVIAND H. (Eds), Numerical Methods for the Computation of Inviscid Transonic Flows with Shock Waves, Notes on Numerical Fluid Mechanics, vol 3, Vieweg, Braunschweig (1981).

28  SELLS C.C.L., Plane Subcritical Flow Past a Lifting Aerofoil, Proc. Roy. Soc., Serie A, vol 308 (1968), pp 377-401.

29  SERRIN J., Mathematical Principles of Classical Fluid Mechanics, in Handbuch der Physics, (Truesdell ed.), Springer Verlag, Berlin, vol 8-1 (1950), pp 125-263.

30  SMOLLER J., Shock Waves and Reaction-Diffusion Equations, Springer Verlag, Berlin (1983).
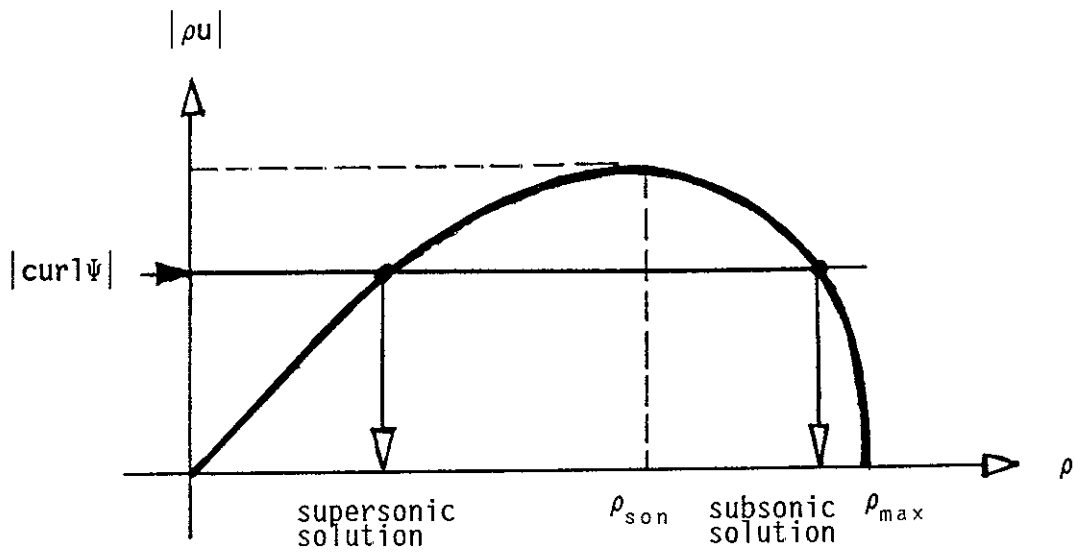
Figure 1   Momentum $|\rho u|$ as a function of the density $\rho$ according to isenthalpy and isentropy hypotheses. A given value of $|\text{curl}\,\Psi|$ corresponds to **two** possible values of the density.
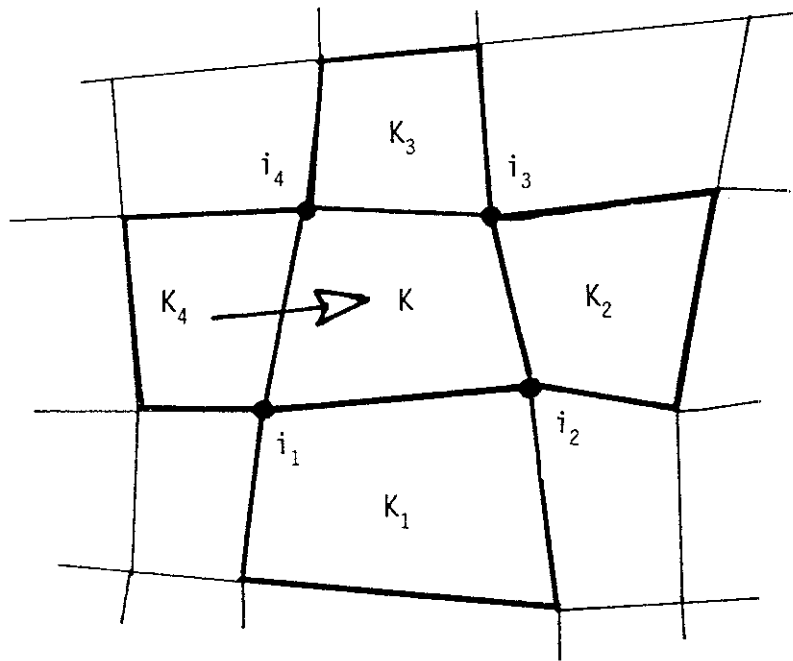
Figure 2    Neighbouring quadrangles $K_1, K_2, K_3$ and $K_4$ of a given finite element K. The **upwind element** KA(K) realizes the maximum of the incoming mass flux accross the four edges of K.
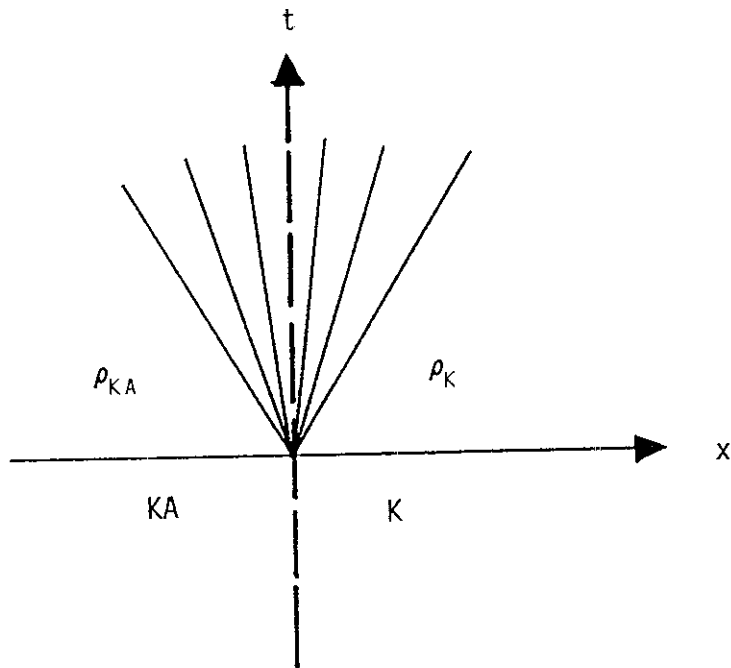
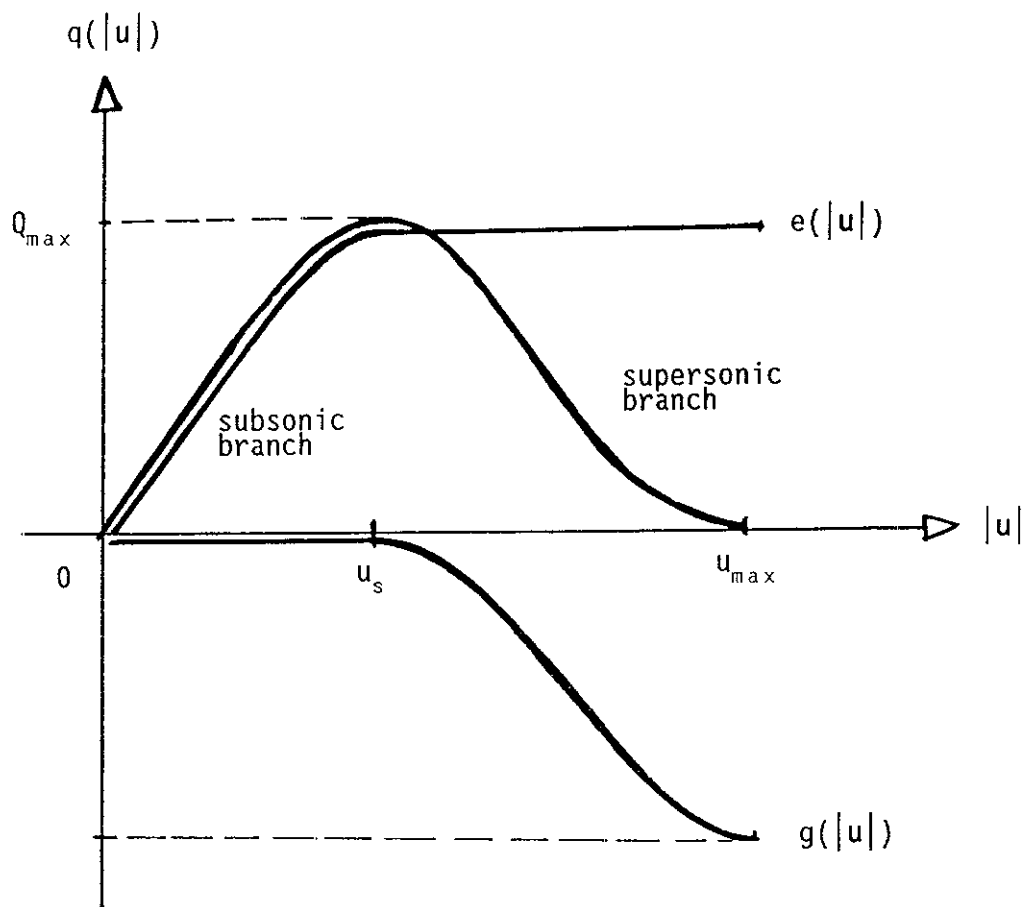Figure 3    Riemann  problem  associated  with  the  upwinding between the
elements K and KA.

**Figure 4** The Engquist-Osher decomposition (2.29) of the nonlinear function q(u) (cf (2.26)).
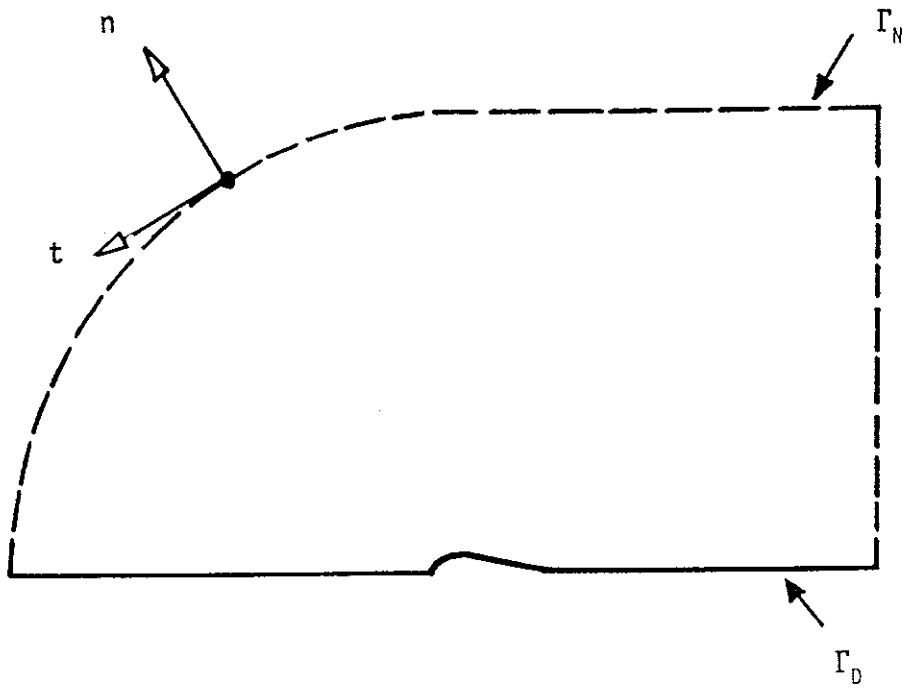
Figure 5    Boundary conditions for the computation of a nonlifting two-dimensional profile. On $\Gamma_D$, the stream function is given by the relation (2.12) and on the portion $\Gamma_N$ of the boundary, the tangential component of the velocity is given by the equation (2.13).
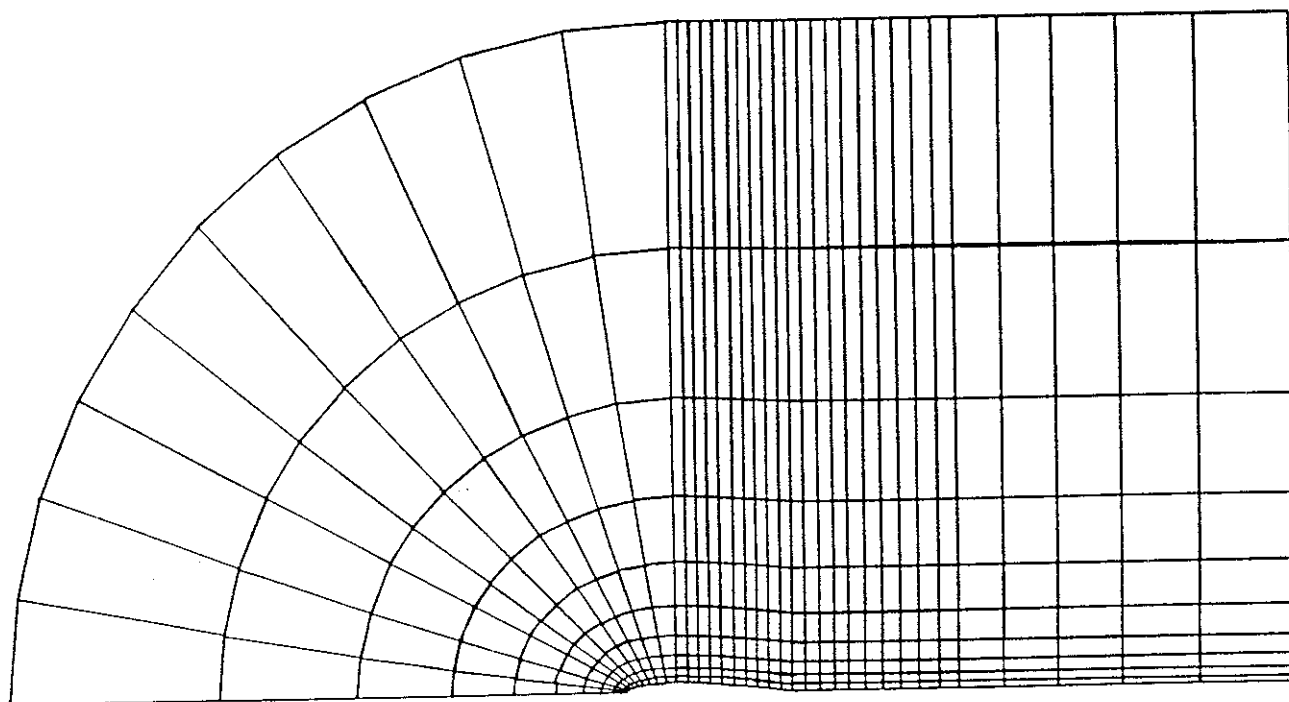
**Figure 6**    View of the mesh for the computations around a nonlifting NACA
0012 wing (36*11 vertices, 21 points on the profile).
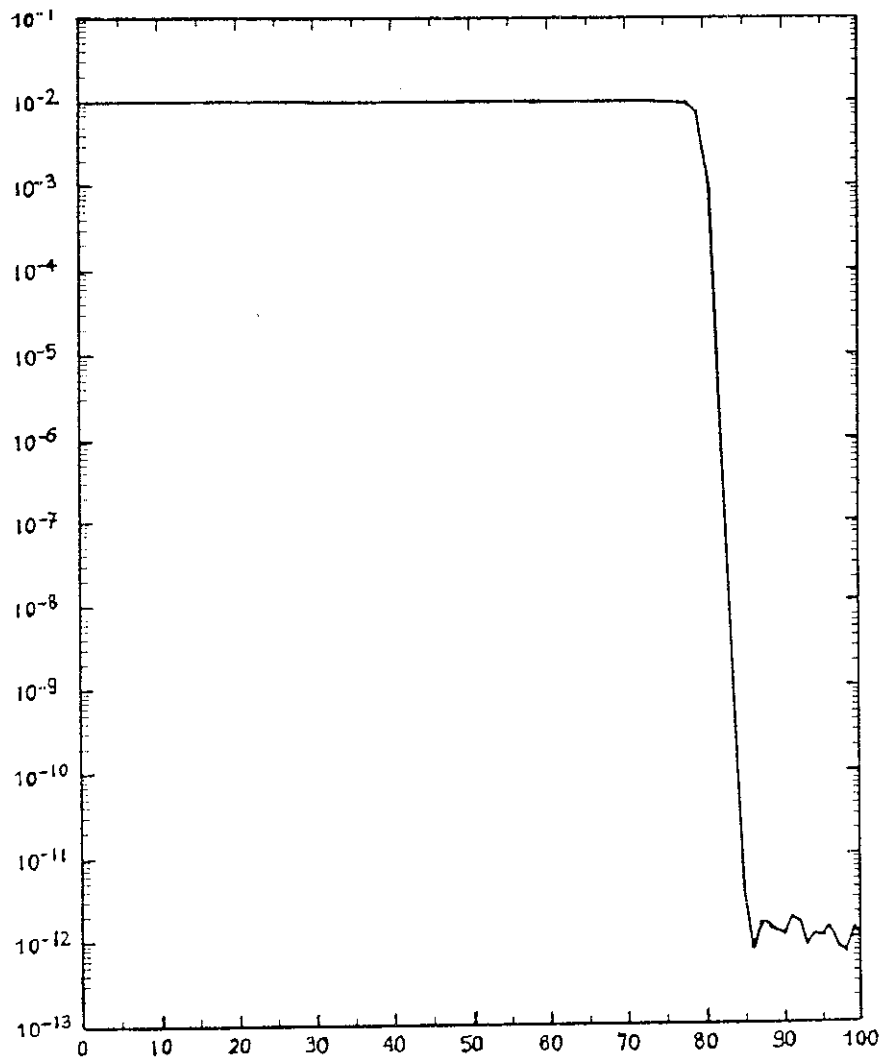
Figure 7        Residual (4.2) of the density during the iterations 250 to 350
                of the algorithm (3.4)-(3.6) for the test case $M_\infty = 0.90$.
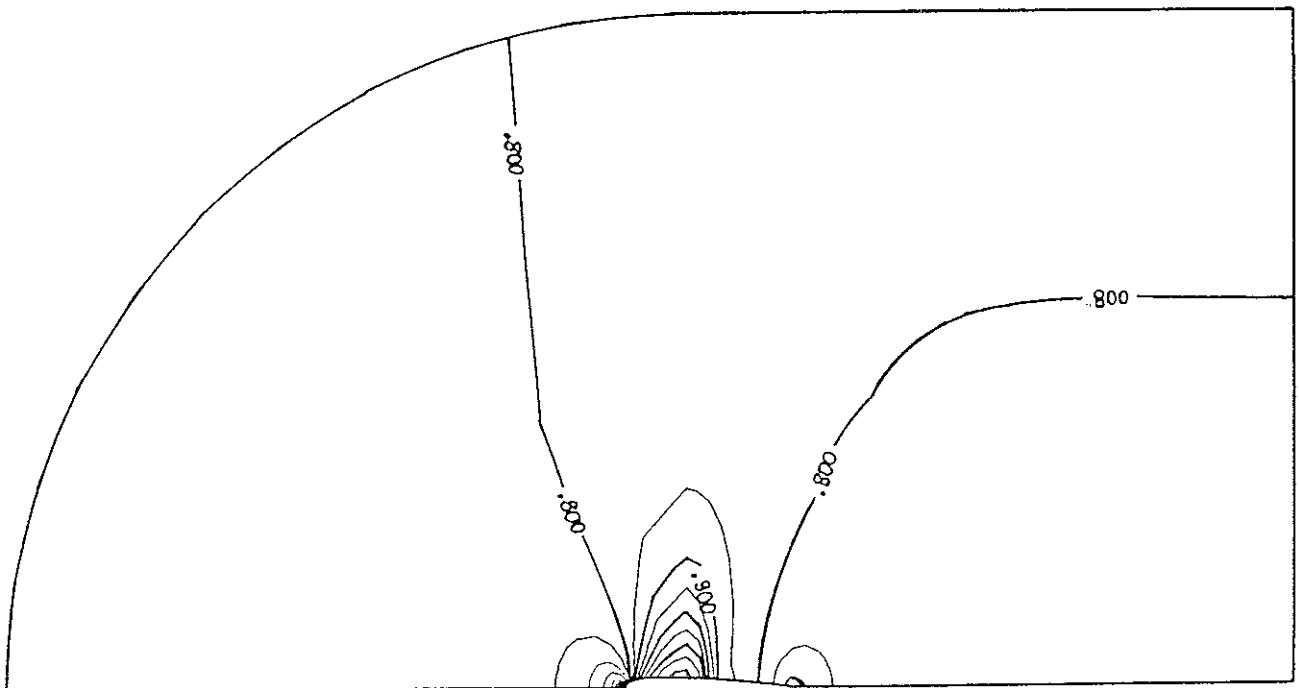
**Figure 8**    Mach number contours for NACA 0012 at $M_\infty = 0.80$
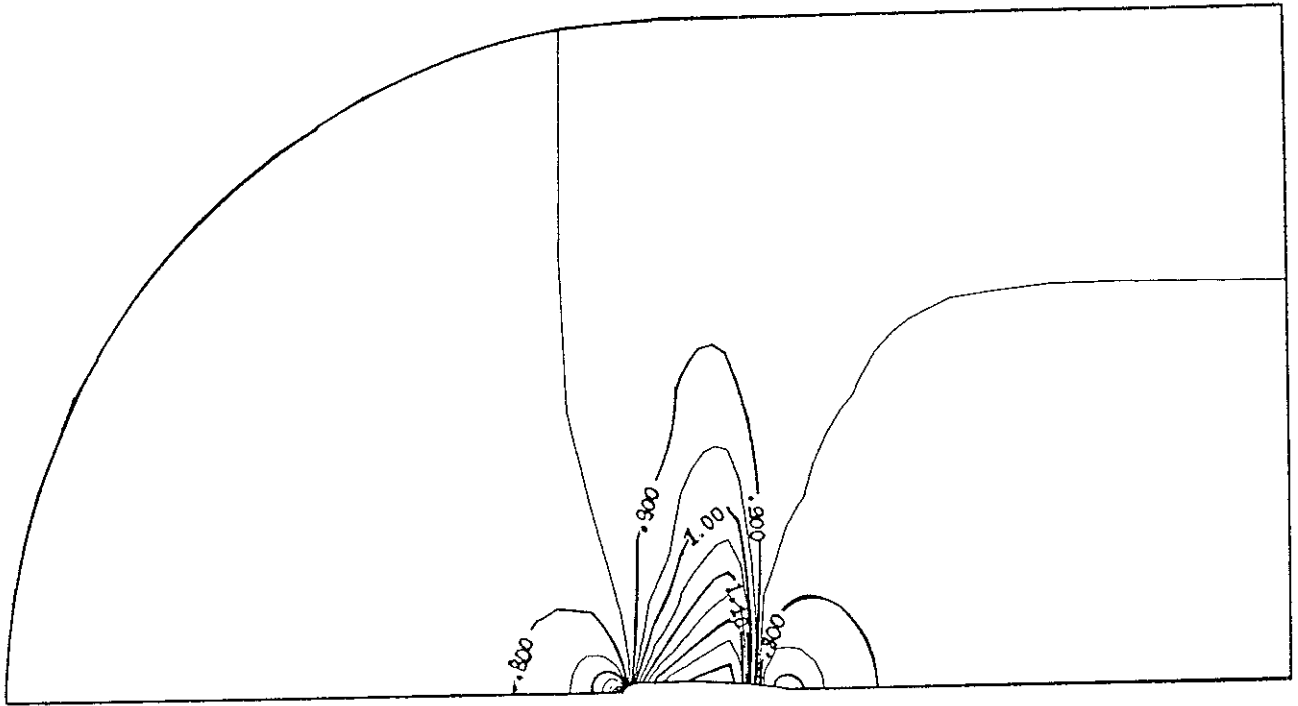
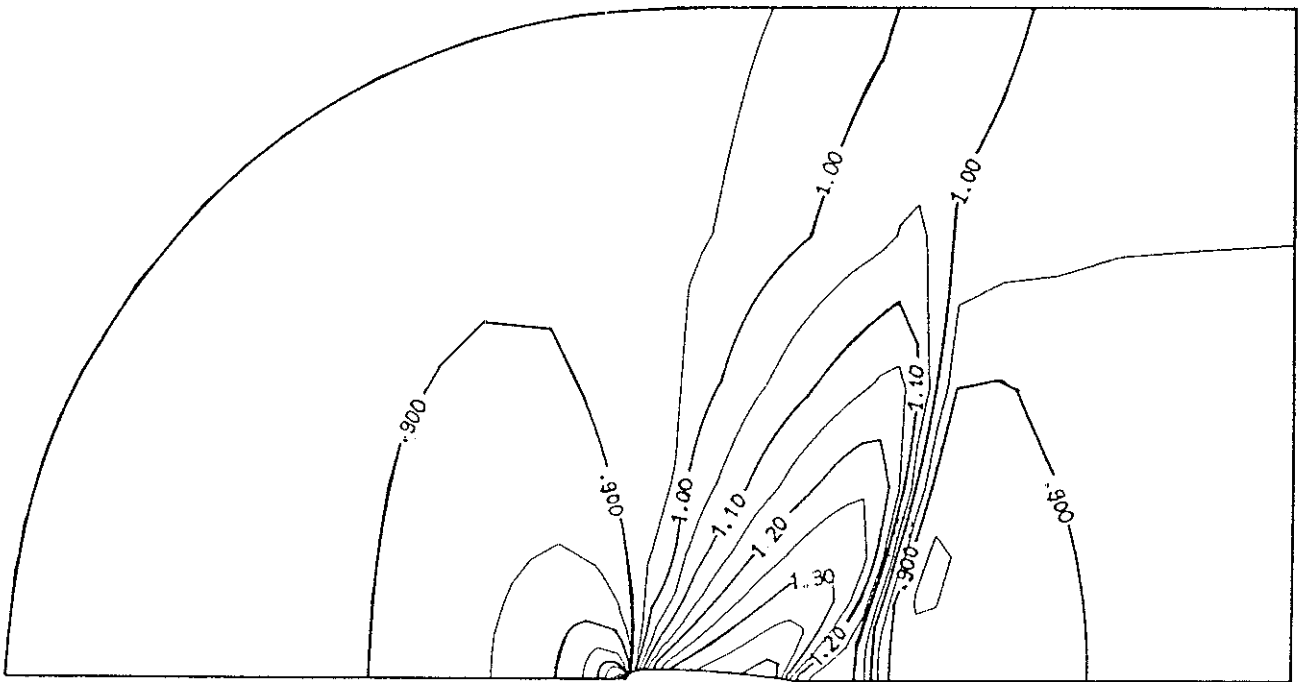Figure 9     Mach number contours for NACA 0012 at $M_\infty = 0.85$
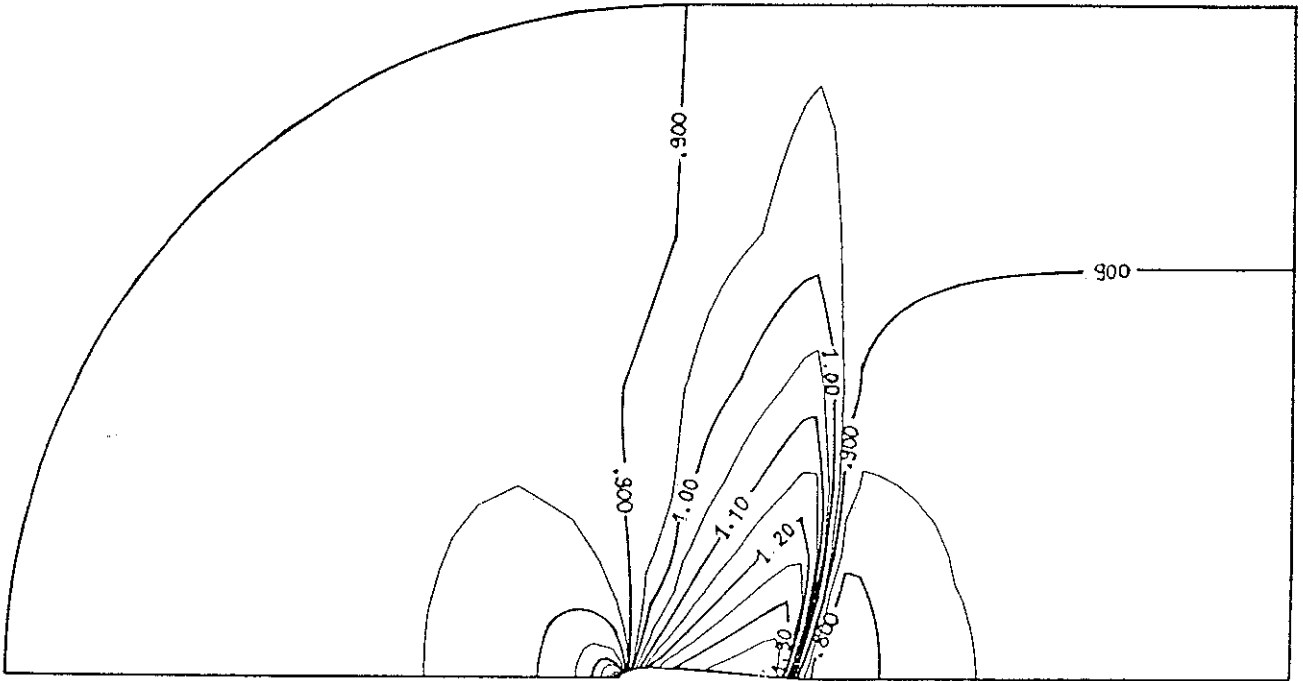
**Figure 10**     Mach number contours for NACA 0012 at $M_\infty = 0.90$

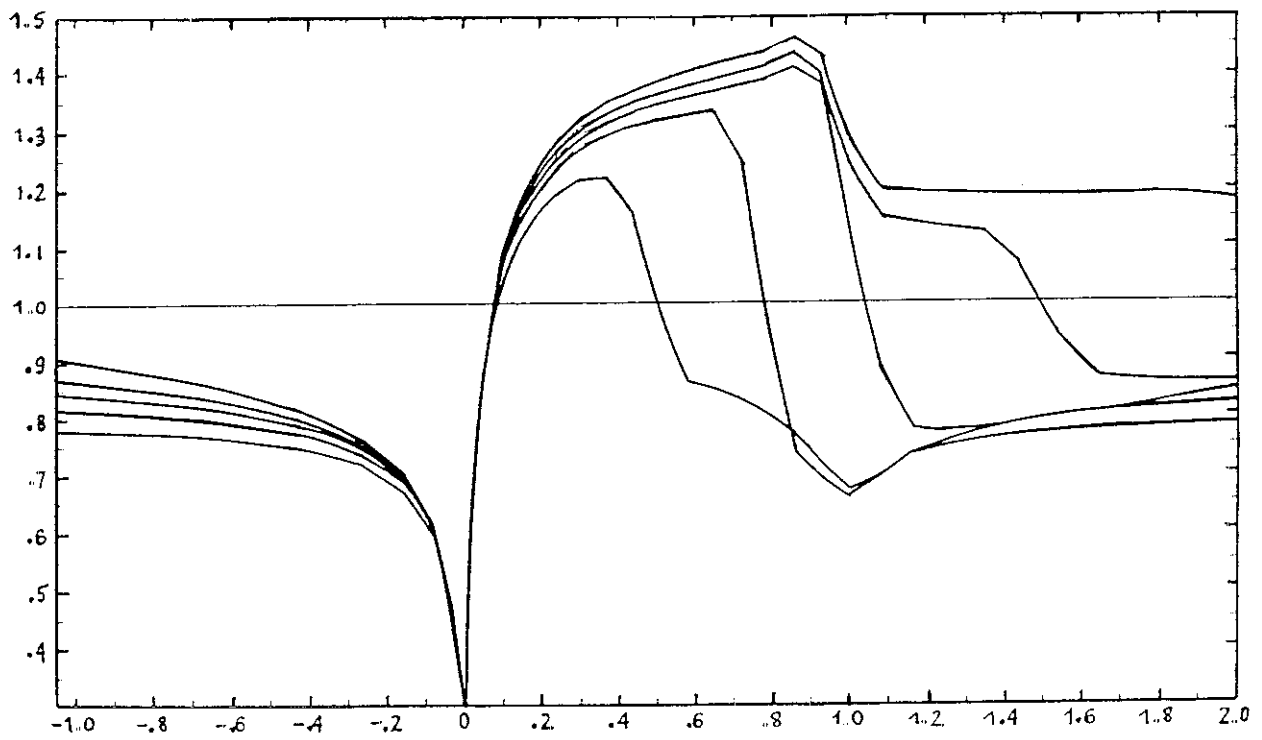Figure 11    Mach number contours for NACA 0012 at $M_\infty = 0.95$

Figure 12    Synthesis of the results (NACA 0012) for the range 0.80 to
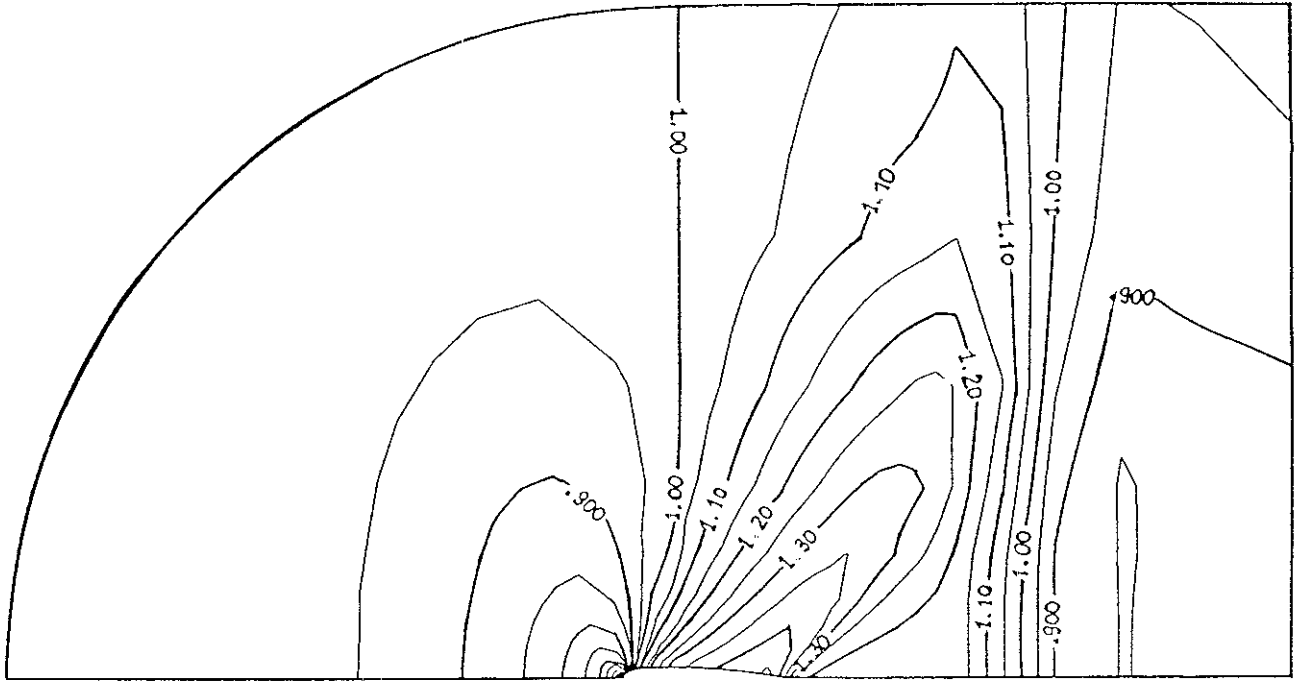1.00 of Mach numbers.

Figure 13    Mach number contours for NACA 0012 at $M_\infty = 1.00$
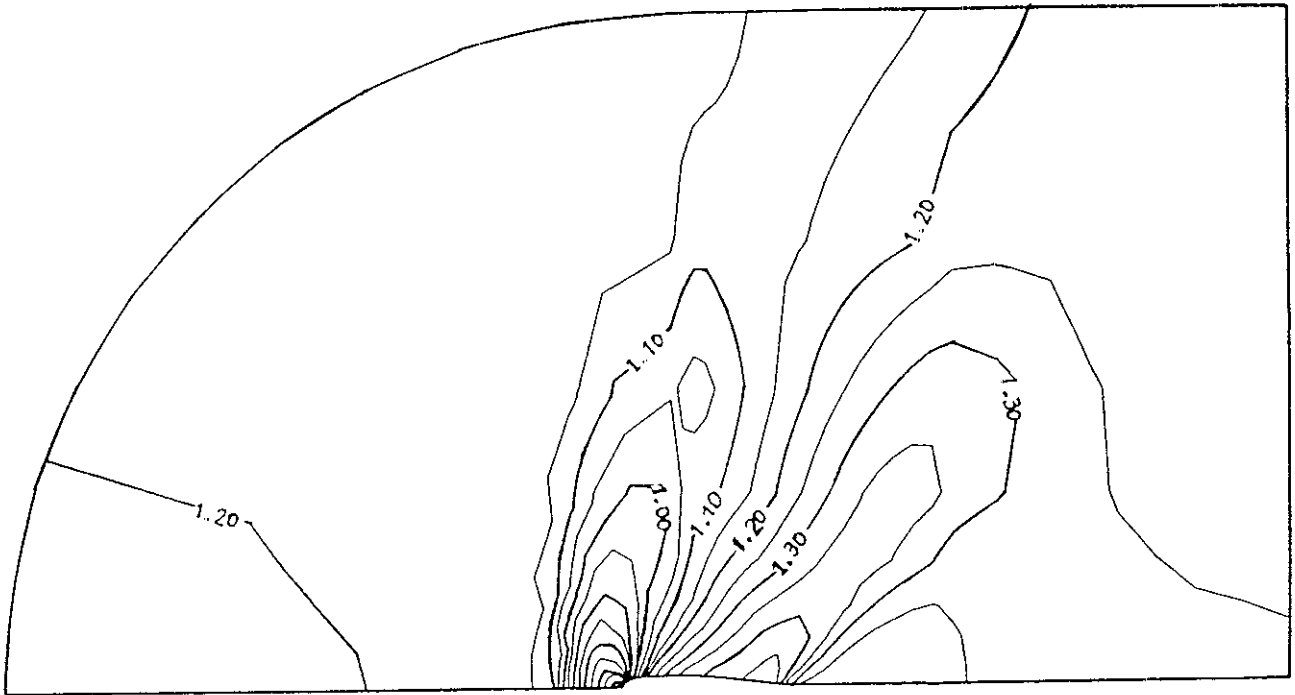
Figure 14    Mach number contours for NACA 0012 at $M_\infty$ = 1.05

Figure 15    Mach number contours for NACA 0012 at $M_\infty = 1.10$

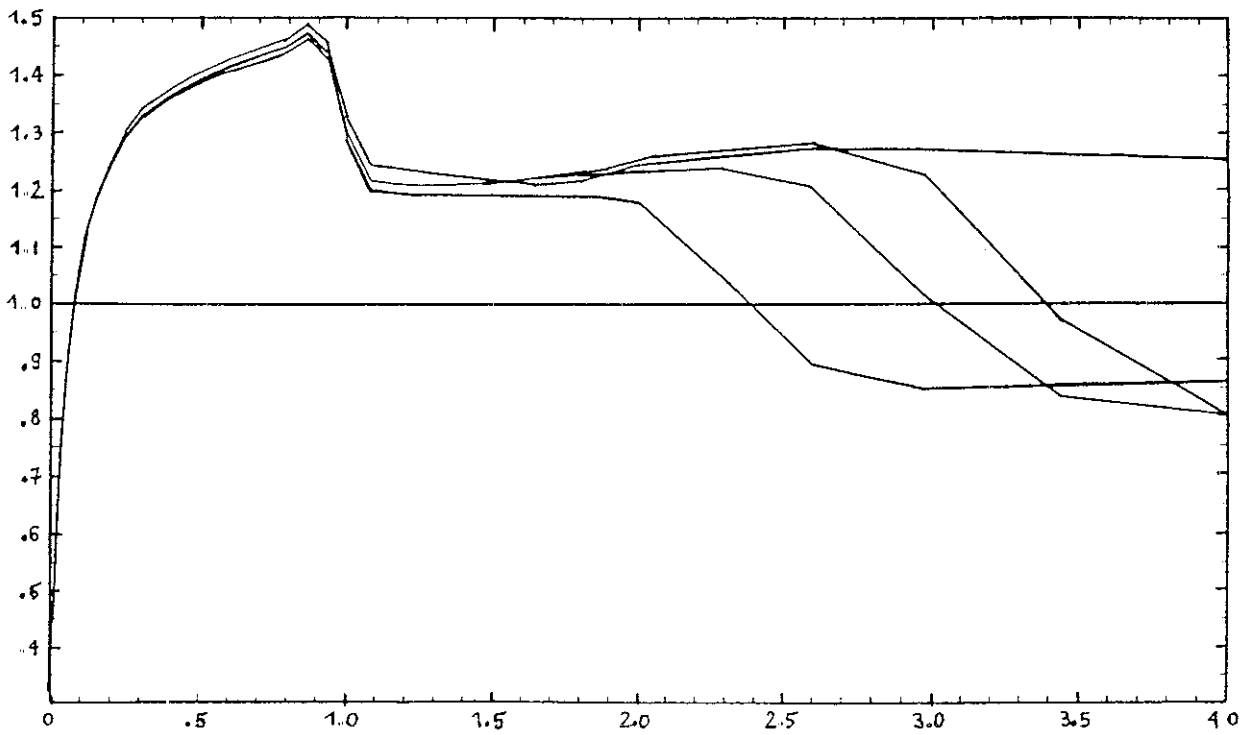Figure 16    Mach number contours for NACA 0012 at $M_\infty = 1.20$

**Figure 17**    Synthesis of  the results   (NACA 0012)   for the   range 1.00 to
1.20 of Mach numbers.